Journal of Geophysical Research: Atmospheres

Supporting Information for

Uncertainty in the response of sudden stratospheric warmings and stratosphere-troposphere coupling to quadrupled CO2 concentrations in CMIP6 models

B. Ayarzagüena[1], A. J. Charlton-Perez[2], A. H. Butler[3], P. Hitchcock[4], I. R. Simpson[5], L. M. Polvani[6], N. Butchart[7], E. P. Gerber[8], L. Gray[9], B. Hassler[10], P. Lin[11], F. Lott[12], E. Manzini[13], R. Mizuta[14], C. Orbe[15], S. Osprey[9], D. Saint-Martin[16], M. Sigmond[17], M. Taguchi[18], E. M. Volodin[19], S. Watanabe[20]

[1] Departamento de Física de la Tierra y Astrofísica, Universidad Complutense de Madrid, Spain

[2] Department of Meteorology, Univ. of Reading, UK

[3] Cooperative Institute for Environmental Sciences (CIRES)/National Oceanic and Atmospheric Administration (NOAA) Chemical Sciences Division, USA

[4] Department of Earth and Atmospheric Sciences, Cornell University, USA

[5] Climate and Global Dynamics Laboratory, National Center for Atmospheric Research, USA

[6] Columbia University, USA

[7] Met Office Hadley Centre, Exeter, UK.

[8] Courant Institute of Mathematical Sciences, New York University, USA

[9] NCAS-Climate, Department of Physics, University of Oxford, UK

[10] Deutsches Zentrum für Luft-und Raumfahrt (DLR), Oberpfaffenhofen, Germany

[11] Atmospheric and Oceanic Sciences Program, NOAA, USA,

[12] Laboratoire de Météorologie Dynamique, Ecole Normale Supérieure, France

[13] Max-Planck-Institut für Meteorologie, Germany

[14] Meteorological Research Institute, Japan

[15] NASA Goddard Institute for Space Studies, USA

[16] Centre National de Recherches Météorologiques (CNRM), Université de Toulouse, Météo-France, CNRS, Toulouse, France

[17] Canadian Centre for Climate Modelling and Analysis Environment and Climate Change, Canada

[18] Department of Earth Science, Aichi University of Education, Kariya, Japan

[19] Marchuk Institute of Numerical Mathematics, Russia

[20] Japan Agency for Marine-Earth Science and Technology (JAMSTEC), Japan

Contents of this file

Introduction

We include one figure and five tables in this supporting information.

Figure S1 shows the composite maps of anomalous SLP (contours) and 2m temperature (shading) after Polar Night-Jet Oscillation (PJO) events averaged over 15/60 days after central date in piControl simulation and JRA-55 simulation (bottom left). Stippling indicates stat. significant differences from JRA-55 reanalysis at the 95% confidence level. Comparing this figure with Figure 7 of the manuscript, we confirm that the tropospheric response to PJOs is stronger than for all sudden stratospheric warmings (SSWs).

Table S1 displays the annual frequency of SSW events in the historical simulations (1958-2014 period) in each model and serves as model validation for simulating SSW events in the historical period. These values are also shown in Figure 1a.

Tables S2 displays information about changes in frequency of SSWs under high CO_2 loading conditions. More specifically, it shows the annual frequency of SSW events in the piControl and abrupt4xCO_2 simulations along with the difference of these frequencies and the statistical information about its significance. Figure 1b is built with this information.

Table S3 shows the standard deviation of daily zonal-mean zonal wind at 10hPa and 60ºN (m s^{-1}) in the piControl and abrupt4xCO_2 simulations.

Table S4 and S5 present information about the trend estimates of SSW frequency and the time of emergence of this trend. Table S4 is complementary to Figure 5a and Table S5 contains the values shown in Figure 5b.

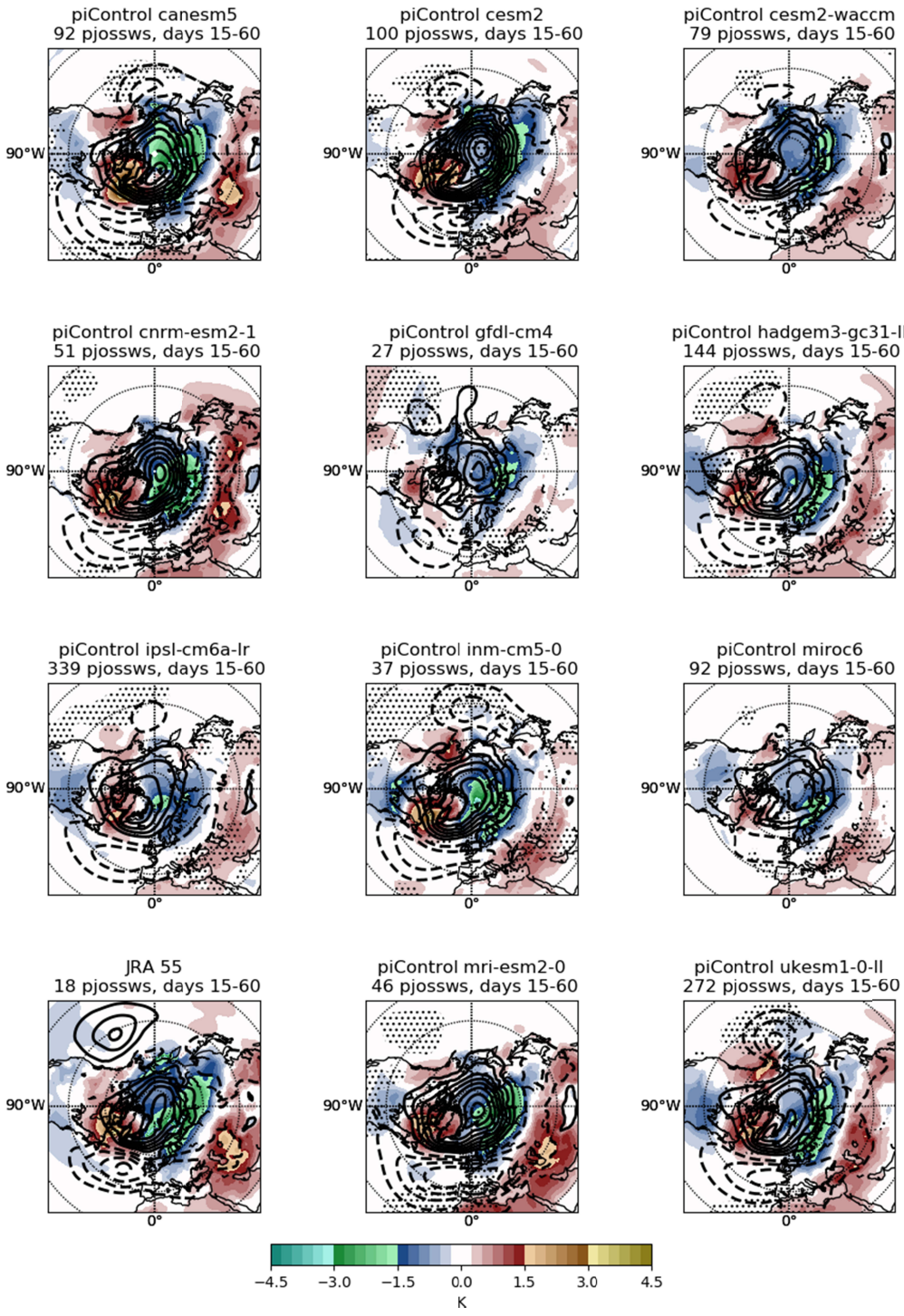

Figure S1. Composite maps of anomalous SLP (contour interval: 1hPa) and 2m temperature (shading, K) after PJOs (averaged over 15/60 days after central date) in the piControl simulation and JRA-55 reanalysis (bottom left). Stippling indicates stat. significant differences from JRA-55 reanalysis at the 95% confidence level.

model	Freq. historical	Difference	p-value (parametric test)	p-value (bootstrapping test)
GFDL-CM4	0.30	-0.33	**0.0087**	**0.0046**
CESM2	0.30	-0.33	**0.0087**	**0.0039**
CanESM5	0.36	-0.28	**0.033**	**0.020**
UKESM1-0-LL	0.48	-0.16	0.27	0.20
INM-CM5-0	0.54	-0.10	0.48	0.37
MIROC6	0.55	-0.09	0.56	0.43
CESM2-WACCM	0.59	-0.05	0.74	0.65
MRI-ESM2-0	0.62	-0.01	0.93	0.85
CNRM-ESM2-1	0.66	0.02	0.88	0.91
HadGEM3-GC31-LL	0.73	0.09	0.54	0.52
IPSL-CM6A-LR	1.00	0.36	**0.032**	**0.0098**

Table S1. Annual frequency of SSW (events per winter) in the historical simulations (period: 1958-2014). The values of the historical frequency are compared with the estimate from the JRA-55 re-analysis (0.64 SSW winter^{-1}). Values in bold indicate that the model SSW frequency is statistically significantly different from JRA-55 one at a 95% confidence level

model	Freq. piControl	Freq. abrupt $4xCO_2$	Difference	p-value (parametric test)	p-value (bootstrapping test)
HadGEM3-GC31-LL	0.75	0.32	-0.44	**$8x10^{-11}$**	**$<1\ x10^{-4}$**
CanESM5	0.45	0.13	-0.32	**$9.3x10^{-11}$**	**$<1\ x10^{-4}$**
IPSL-CM6A-LR	0.76	0.49	-0.27	**$3.3x10^{-15}$**	**$<1\ x10^{-4}$**
INM-CM5-0	0.50	0.34	-0.16	**0.034**	**0.0231**
GISS-E2-2-G	0.25	0.14	-0.11	0.16	0.14
UKESM1-0-LL	0.54	0.48	-0.063	0.33	0.29
GFDL-CM4	0.32	0.38	0.059	0.4	0.31
MRI-ESM2-0	0.48	0.56	0.078	0.32	0.25
CESM2	0.23	0.37	0.14	**0.0031**	**$8\ x10^{-4}$**
CNRM-ESM2-1	0.53	0.69	0.16	**0.026**	**0.007**
MIROC6	0.46	0.67	0.21	**0.0019**	**$<1\ x10^{-4}$**
CESM2-WACCM	0.46	0.80	0.34	**2.8x10-6**	**$<1\ x10^{-4}$**

Table S2. Annual frequency of SSW (events per winter) in the piControl and abrupt$4xCO_2$ simulations along with the difference of these frequencies. Values in bold indicate that the abrupt4xCO2 value is statistically significantly different from the piControl one at a 95% confidence level

model	std. piControl [m s^{-1}]	std. abrupt 4xCO_2 [m s^{-1}]	Difference [m s^{-1}]
HadGEM3-GC31-LL	17.0	16.5	**-0.5**
CanESM5	13.9	11.9	**-2.0**
IPSL-CM6A-LR	14.6	16.9	**2.3**
UKESM1-0-LL	16.9	17.7	**0.6**
GFDL-CM4	11.6	12.3	**0.7**
MRI-ESM2-0	16.3	17.4	**1.1**
CESM2	15.3	17.0	**1.7**
CNRM-ESM2-1	17.1	18.6	**1.7**
CESM2-WACCM	11.7	12.3	**0.6**
MIROC6	14.2	15.8	**1.6**
GISS-E2-2-G	17.1	15.9	**-1.2**
INM-CM5-0	15.7	15.5	**-0.2**

Table S3. Standard deviation of daily zonal-mean zonal wind at 10hPa and 60°N (m s^{-1}) in the piControl and abrupt4xCO_2 simulations. Difference values in bold indicate statistically significant values at a 95% confidence level (Pearson values).

Model	Trend	p-value
CanESM5	**0.96**	0.036
HadGEM3-GC31-LL	**0.96**	0.0045
IPSL-CM6A-LR	0.99	0.27
INM-CM5-0	0.99	0.81
UKESM1-0-LL	1.00	0.94
CESM2	1.02	0.57
MIROC6	1.03	0.14
CNRM-ESM2-1	**1.03**	0.023
CESM2-WACCM	**1.05**	0.034
GFDL-CM4	**1.05**	0.048
MRI-ESM2-0	**1.08**	0.0011

Table S4. Trend estimates of SSWs for the 1pctCO2 runs. The trend is expressed in terms of the fractional change in SSW frequency per decade.

Model	Trend	Decade of Emergence
MRI-ESM2-0	1.08	4
CESM2-WACCM	1.05	8
GFDL-CM4	1.05	9
HadGEM3-GC31-LL	0.96	11
CNRM-ESM2-1	1.03	11
CanESM5	0.96	14

Table S5. Decade of emergence of the trend of SSWs for models where the trend is significant based on Table S4.